Designing of a fuzzy-sliding mode Controller for UPFC to Improve the Transient Stability

Mohsen Azizi[1], Amir Hossein Zaeri[2], Mohammad Reza Zareh[3]
1-Department Of Electerical Engineering, Majlesi Branch, Islamic Azad University, Isfahan, Iran
E-mail:Mohsen.Azizi62@yahoo.com (Corresponding author)
2-Department of Electerical Engineering, Majlesi Branch, Islamic Azad University, Isfahan, Iran
E-mail: amzaeri@gmail.com
3-Department of Electerical Engineering, Majlesi Branch, Islamic Azad University, Isfahan, Iran
E-mail: zareh81@gmail.com

Abstract: An UPFC may be applied for steady-state power-flow and voltage control as well as for mastering dynamic phenomena like transient-stability margin enhancement, oscillation damping, etc. For these tasks the Lyapunov energy-function approach is frequently used as a convenient way to control or analyze the electric-power system (EPS). The basis for the implementation of such an approach is to know the energy function of the EPS. Currently, this is not possible for the EPSs that include UPFCs, because the already known energy functions that proved to be suitable for an EPS do not include such a device. In the present paper, the convenient operation and control of UPFC for transient stability improvement are considered. Considering that the system's Lyapunov energy function is a relevant tool to study the stability affair. UPFC energy function optimization has been used in order to access the maximum of transient stability margin. In order to control UPFC, a fuzzy-sliding mod (FSM) and PI controller have been used. The designing results have been studied by the simulation of a single-machine system with infinite bus (SMIB) and another standard 9-buses system (Anderson and Fouad, 1977).

1. Introduction

With the increased importance of online dynamic security assessment the Lyapunov direct method might be applied to avoid the time-consuming repetition of solving a system's nonlinear differential

equations in a step-by-step manner. However, to apply this direct method one has to have the proper Lyapunov function for the electric-power system (EPS). Although many different Lyapunov functions have been constructed for a system without FACTS devices, the function obtained by integrating a system's swing

equations and thus representing the sum of the kinetic and potential energies has provided the best results [1]. Instabilities in power system are caused by insulation breakdown or collapse, long length of transmission lines, interconnected grid, changing system loads and other unforeseen disturbances in the system. These instabilities result in reduced line flows or even line trip. FACTS devices stabilize transmission systems with increased transfer capability and reduced risk of line trips. Other benefits attributed to FACTS

devices are additional energy sales due to increased transmission capability, reduced wheeling charges due to increased transmission capability and due to delay in investment of high voltage transmission lines or even new power generation facilities. These devices stabilize transmission systems with increased transfer capability and reduced risk of line trips [1]. The major problem in power system is upholding steady acceptable system parameters like bus voltage, reactive power and active power under normal operating and anomalous conditions. This is usually system regulation problem and regaining synchronism after a major fault is critical for this phenomenon. Faults can cause loss of synchronism. As effects of instability, faults occur due to insulation breakdown or compromise as result of lightning ionizing air, power cables blowing

In [1], together in the wind, animals or plants coming in contact with the wires, salt spray, pollution on insulators, system overloading, long transmission lines with uncontrolled buses at the receiving end, shortage of local reactive power, intrinsic factors, natural causes

like harsh weather and small generation reserve margins. Such system disturbances have led to the introduction of FACTS devices such as SVC, SSSC, STATCOM, UPFC and IPFC [2,3], also, has considered transient stability improvement using UPFC. It has been accomplished a lot of studies on UPFC, simulation, and modeling. [4], is among the other fundamental works which has done the simulation and modeling of UPFC in MATLAB and EMTP. [5], also, has considered UPFC discontinuous control by maximizing and minimizing the line power flow via UPFC and by the aim of transient stability improvement. The application of the direct method of Lyapunov stability has been studied in 1980s [6]. [7], is the basis of many studies accomplished in applying Lyapunov function in the power networks despite FACTS devices. In [8], with the aim of accessing to maximum of the transient stability limit, the maximization of the network total potential energy has been considered by defining the critical energy function for UPFC and controlling it adequately. Also, there are some studies relating to the application of the Lyapunov direct method for controlling UPFC with the aim of damping the system oscillations [9]. In [10], UPFC intellectual control has been studied via designing two fuzzy controllers. One controller was used for calculating essential power for transient stability improvement, and the other for controlling UPFC parameters with the aim of producing the calculated power. In some papers, the application of Neuro networks in controlling FACTs devices, such as UPFC, has been studied [11]. In [12, 13], it is considered controlling UPFC by Nero network based on Lyapunov in order to improve power system transient stability. In [14], SSSC, STATCOM, and UPFC have been controlled by the radial basis function network (RBFN) controller, and their function has been compared in transient stability improvement.

According to the review in [15], several attempts have been made to model the emotional behavior of the human brain [16], [17]. In [17], the computational models of the amygdala and context processing were introduced, which were named Brain Emotional-Learning (BEL) model, which was not used in any practical area, particularly in engineering applications. Based on the cognitively motivated open-loop model, the BEL-based intelligent controller (FSM) was introduced for the first time by Lucas in 2004 [18], and during the past few years, this controller has been used in control devices for several industrial applications such as heating, ventilating, and air conditioning control problems, washing machines, controlling a mobile crane and electrical machine drives [19]–[25]. The main features of that controller were its enhanced learning capability, provision of a model-free control algorithm, robustness, and ability to respond swiftly.

For the first time, the implementation of the FSM method for electrical drive control was presented by Rahman et al. [26]. In [27], Markadeh et al, used a modified emotional controller for the simultaneous speed and flux control of a laboratory IM drive. This simultaneous speed and flux control is achieved by quick auto learning and adaptively proper tracking of reference speed and is quite independent of system parameters, which results in performance improvement.

Moreover, many other advantages of the FSM are investigated in other electric drives in [28]. [29], is the only paper which study the application of FSM on the power system.

2. Modeling of System
2.1. Unified power flow controller(UPFC)

UPFC was established to create a multi-application flexibility for solving many problems of the power transmission industry. In the framework of the traditional concepts of the power transmission, UPFC is capable to control all parameters synchronically or adoptively affecting on the power flow in transmission line (that is, voltage, impedance, phase angle).
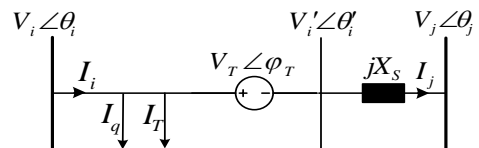

Fig.1. UPFC fundamental model

Furthermore, it can separately control the flow of both active and reactive powers on the line. In an ideal system, UPFC can be displayed with a series voltage source via the reactance (X_s) related to UPFC's transformer and a current source with shunt connection [8].

This configuration has been shown on figure (1). In this figure, UPFC has placed between

2

buses i and j. The current (I_T) is in phase with (V_i) and shows the real power exchanged between the series and shunt branch. This power is the same power which is injected to the power network via the series branch. (Iq) shows the shunt reactive branch which is independent from (V_i).

UPFC controllable parameters contains: the series branch voltage value (V_T), series branch voltage angle $(\ddot{o}_T)$ toward the bus voltage (V_i), and series branch reactive current (Iq). The active current (I_T) depends on the real power that the series branch will inject to the network. In the other words, its value is determined so that the real power balance can be confirmed between series and shunt branch.

Figure (2) shows UPFC phasor diagram representing its series and shunt branch as the magnitude and angle of series branch voltage $(V_T$ and $\ddot{o}_T)$ and series branch current $(I_T$ و $I_q)$ with the vectors of the network current and voltage. Figure (3) shows the injecting power of series branch. This model resembles to SSSC injecting model that we can derive the equations related to UPFC by adding the shunt branch.

$$P_{si} = \frac{V_i V_T}{X_S} \sin(\varphi_T) + V_i \cdot I_T \qquad (1)$$

$$P_{sj} = -\frac{V_j V_T}{X_S} \sin(\theta_{ij} + \varphi_T) \qquad (2)$$

$$Q_{si} = \frac{V_i \cdot V_T}{X_S} \cos(\varphi_T) + V_i \cdot I_q \qquad (3)$$

$$Q_{sj} = -\frac{V_j \cdot V_T}{X_S} \cos(\theta_{ij} + \varphi_T) \qquad (4)$$

Where, $\grave{e}_{ij} = \grave{e}_i - \grave{e}_j$

Now, the modeling can be continued considering the real power balance between series and shunt branch. As pointed before, I_T is the real part of the series branch current. Also, in the shunt branch, the real part of the complex power shows the injecting real power, so:

$$V_i \cdot I_T = Re[V_T \cdot I_j^*] \qquad (5)$$

By deriving (Ij):

$$I_j = \left(\frac{\acute{V}_i - V_j}{jX_S}\right) \qquad (6)$$

Attending to the phasor diagram in figure (٢), the magnitude and angle of the voltage $\acute{V}_i$ can be written as following

$$|\acute{V}_i| = \sqrt{(V_i + V_T \cos(\varphi_T))^2 + (V_T \sin(\varphi_T))^2}$$

$$(7)$$

$$\angle(\acute{V}_i) = \theta_i + \arctan \qquad (8)$$

Replacing the obtained equations, and after the simplification, the real power is calculated as following

$$V_i \cdot I_T = \frac{V_j V_T}{X_S} \sin(\theta_{ij} + \varphi_T) - \frac{V_i V_T}{X_S} \sin(\varphi_T)$$
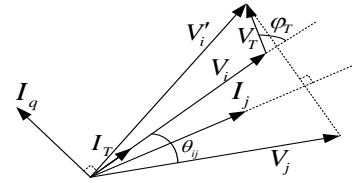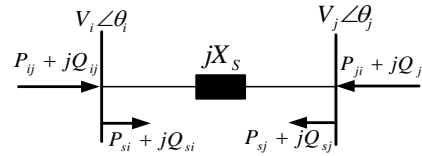
$$(9)$$

Fig .2. Phasor diagram

Fig.3. UPFC injected powers model

By replacing it on the equation (1), Hence:

$$P_{si} = \frac{V_i V_T}{X_S} \sin(\theta_{ij} + \varphi_T) = -P_{sj} \qquad (10)$$

This relation, by mathematical analyzing, affirms the real power balance in UPFC, it means:

$$P_{si} + P_{sj} = 0 \qquad (11)$$

Thus, the basic relations concerning UPFC, which are necessary on the next stages and during the control operations, were derived [8].

2.2. Energy Function

In [8] and [11], it has been affirmed if UPFC, depending on its rated values, could

3

have the maximum magnitude of V_T and I_q, the maximum transient stability margin will be obtainable. So, if V_T and I_q are set in their maximum value and φ_T is fixed, UPFC Lyapunov energy function will be definable for the first oscillation.

In order to deriving the system energy function with UPFC, it is used of the SPEF method [7]. The classic model is also considered for the generator. The loads are also modeled as the fixed admittance. The energy function of the whole system, containing N bus and m generator, is calculated as following:

$$V_{SPEF}(\widetilde{\omega}, \widetilde{\phi}, V) = V_k(\widetilde{\omega}) + V_{p1}(\widetilde{\phi}, V) + V_{p2}(\widetilde{\phi}) + K \qquad (12)$$

In which:
$$\widetilde{\phi} = [\widetilde{\delta}^T, \widetilde{\theta}^T]^T \qquad (13)$$

And δ is a vector consisting of the rotor angles of m generator; θ is a vector consisting of the voltage angles of N bus; $\grave{u}$ is a vector consisting of the rotor speed of the m generator; and V is vector consisting of the voltage magnitude of N bus. The symbol (~) over the variables has been written to present the variables toward the Center Of Angle (COA) frame. K is an optional constant which is usually set so that it sets the equation source on Zero. V_k is the kinematical energy, and the remaindering of the terms is the system potential energy; thus V_{p2} is the potential energy of the system loads, and V_{p1} is defined as following:

$$V_{p1}(\widetilde{\phi}, V) = -\sum_{i=1}^{m} P_{mi} \widetilde{\phi}_i + \sum_{i=m+1}^{m+N} \int \frac{Q(V_i)}{V_i} dV_i - \frac{1}{2} \sum_{i=1}^{m+N} \sum_{j=1}^{m+N} B_{ij} V_i V_j \cos \widetilde{\phi}_{ij} \qquad (14)$$

In this equation, P_{mi} is input mechanical energy of machine i, $Q(V_i)$ is the reactive part related to bus voltage i, B_{ij} is the susceptance in the increased admittance matrix.

If UPFC injected real power, that is P_{si} and P_{sj}, is multiplied by $\dot{e}_i$ and $\dot{e}_j$, and then their outcome is added up, Hence:

$$P_{si}\dot{\theta}_{ij} = \frac{V_i V_T}{X_S} \sin(\theta_{ij} + \varphi_T)\,\dot{\theta}_{ij} \qquad (15)$$

Now, the equation (3) is multiplied by $\dot{V}_i$, and then is divided by V_i; and the equation (4) is multiplied by $\dot{V}_j$, and then is divided by V_j:

$$\frac{Q_{si}}{V_i}\dot{V}_i = \frac{\dot{V}_i V_T}{X_S} \cos(\varphi_T) + \dot{V}_i \cdot I_q \qquad (16)$$

$$\frac{Q_{sj}}{V_j}\dot{V}_j = -\frac{\dot{V}_j V_T}{X_S} \cos(\theta_{ij} + \varphi_T) \qquad (17)$$

The following outcome is obtained from the sum total of the equation (15) to (17):

$$\frac{V_T}{X_S} \cdot \left[V_j\, sin(\theta_{ij} + \varphi_T)\dot{\theta}_{ij} + \dot{V}_i\, cos(\varphi_T) - \dot{V}_j\, cos(\theta_{ij} + \varphi_T)\right] + \dot{V}_i \cdot I_q \qquad (18)$$

Now, the integral of these relations must be calculated. But there is no identical way for calculating such integrals. There is a specific way for solving each of FACTS devices depending on the controllable strategy. Here, if V_T و I are set on their maximum value, and $\ddot{o}_T$ be a Sectional Constant, the equation (18) can be defined as following:

$$\frac{d}{dt}\left[\frac{V_T}{X_S}\left(V_i \cos(\varphi_T) - V_j \cos(\theta_{ij} + \varphi_T)\right) + V_i \cdot I_q\right] \qquad (19)$$

Now, UPFC Lyapunov energy function can be obtained as an explicit function in the form of $V_{UPFC} = f(V_i, V_j)$ via integration of the equation (19). So, UPFC potential energy is calculated as following:

$$V_{UPFC} = \frac{V_T}{X_S}\left(V_i \cos(\varphi_T) - V_j \cos(\theta_{ij} + \varphi_T)\right) + V_i \cdot I_q \qquad 20)$$

This energy function is the sum total of reactive powers Q_{si}, Q_{sj} according to figure (3), and is the indicant of the whole reactive power injected to the system by UPFC. In the case of SSSC and UPFC, the energy function is the total of the active powers [8]:

$$V_{(UPFC,SSSC)} = Q_i + Q_j \qquad (21)$$

By deriving UPFC energy function, it can be added to energy function of the whole network (the equation (12)), so [8]:

4

$$V_{SPEF}(\widetilde{\omega}, \tilde{\phi}, V) = V_k(\widetilde{\omega}) + V_{p'}(\tilde{\phi}, V) +$$
$$V_{p'}(\tilde{\phi}) + V_{UPFC}(\tilde{\phi}) + K \qquad (22)$$

3. Control method

As pointed previously, when the purpose is transient stability improvement, two controllable parameters V_T and I_q must be set in their maximum value proportional to the selective rated values; in the other words, after selecting UPFC rated voltage and power, two parameters from three controllable parameters will be marked. So, it just remains parameters $ö_T$. On the other hands, the more energy UPFC injects to the network, the more transient stability security margin will be. Thus, use UPFC energy function is used to control UPFC optimally at the purpose of transient stability. In this way that $ö_T$, be determined so that UPFC energy function would be maximized in Eq. (20). As, for obtaining φ_T, by which the energy function is maximized, the derivative of the energy function should be done towards $ö_T$.

$$\frac{dV_{UPFC}}{dö_T} = 0 \qquad (23)$$

$$\frac{V_T}{X_S}(-V_i\sin(ö_T) + V_j\sin(è_{ij} + ö_T)) \qquad (24)$$

If $X_S = 0.1\, P.U$, $V_j = 1 P.U$, $è_{ij} = è_i = ä$, hence: $\qquad (25)$

$-U_i\sin(ö_T) + \sin(ä + ö_T) = 0 \qquad (26)$
$ö_T$ is calculated by (31).

$$ö_T = -\frac{i}{2}\log[\frac{U_i - e^{-äi}}{U_i - e^{äi}}] \qquad (27)$$

And, according to Eq. (11) and Eqs. (1) and (2),

$$V_i\sin(ö_T) - V_i\sin(ö_T + ä) + V_iI_T = 0 \qquad (28)$$

If $ö_{T1}$, be clear then I_T is also calculated.

3.1. FUZZY SLIDING MOD
Fig. (8-a) shows the UPFC connected with the single machine infinite bus (SMIB) system Voltage at the generator terminal is $V_1\angle\delta$, impedance of the tieline and series connecting transformer is $r_{se}+jx_{se}$, impedance of shunt connecting transformer is rs+jxs, and voltage at the bus is $V_b\angle\theta$. Current from the generator is i_s, current exchanged by shunt converter is and current flowing through series converter is i_{se}. The respective subscripts d and q represents the direct and quadrature axis components. Fig. (8-b) shows the vector diagram of different voltages in d-q reference frame. The mathematical structure of SMIB with UPFC used in the paper is based on dq0 reference frame.

With the higher modelling of synchronous generator the accuracy of the system increases, but it also increases the system complexity.
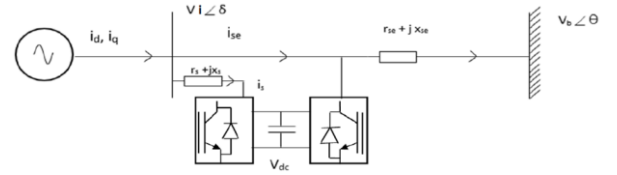

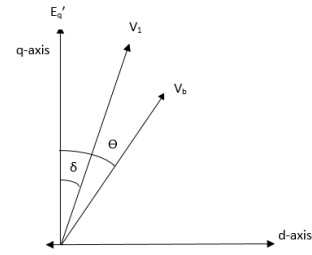**Fig. (8-a)**. Single Machine Infinite Bus System with UPFC

Fig. (8-b). Vector diagram of voltages in d-q reference frame

With the higher modeling of synchronous generator the accuracy of the system increases, but it also increases the system complexity. So to maintain the required accuracy andavoid system complexities we have used fourth order model of synchronous generator, by neglecting the effect of the damper winding as illustrated in reference [10]. The generator data is taken from reference [11].

The UPFC is modeled with two voltage source converters (VSC) one in shunt and other in series with the tie line, both the converters are linked through a DC link capacitor, in order to maintain voltage support for the converters and provide independent control for real and reactive powers by the two converters. In UPFC both the converters are able to exchange real and reactive power with the power system, but in our system we have used series converter to exchange the real and reactive power and shunt converter has been used to exchange the real power demanded or

absorbed by the series converter to keep the DC link capacitor voltage
constant. The mathematical structure for the UPFC has been used as described in reference [12] and is given as follows:

Shunt Converter

$$\frac{d}{dt}\begin{bmatrix} i_{sed} \\ i_{seq} \end{bmatrix} = \begin{bmatrix} \dfrac{-r_{se}}{L_{se}} & \omega \\ -\omega & \dfrac{-r_{se}}{L_{se}} \end{bmatrix}\begin{bmatrix} i_{sed} \\ i_{seq} \end{bmatrix} + \begin{bmatrix} \dfrac{1}{L_{se}} & 0 \\ 0 & \dfrac{1}{L_{se}} \end{bmatrix}\begin{bmatrix} V_d + e_{sed} - V_{bd} \\ V_q + e_{seq} - V_{bq} \end{bmatrix}$$

(29)

Series Converter

$$\frac{d}{dt}\begin{bmatrix} i_{sd} \\ i_{sq} \end{bmatrix} = \begin{bmatrix} \dfrac{-r_s}{L_s} & \omega \\ -\omega & \dfrac{-r_s}{L_s} \end{bmatrix}\begin{bmatrix} i_{sd} \\ i_{sq} \end{bmatrix} + \begin{bmatrix} \dfrac{1}{L_s} & 0 \\ 0 & \dfrac{1}{L_s} \end{bmatrix}\begin{bmatrix} V_d - e_{sd} \\ V_q - e_{sq} \end{bmatrix}$$

Where:

$i_q = i_{sq} + i_{seq}$, $V_i = V_d + V_q$

(30)

The DC link capacitor voltage dynamics has been established on the basis of power balance on the DC side of the converters. The net real power exchanged by both the converters through DC side should be zero to keep the capacitor voltage constant.

A. Sliding Mode Control

The sliding mode control is popular nonlinear control technique which is known for its robustness against parameter variations. The SMC based controller brings the system to steady state by sliding the state trajectory along the sliding surface and reducing the error value to zero, when the state trajectory reaches to origin. This sliding surface is usuallydefined by using the error and its derivative as in (12).
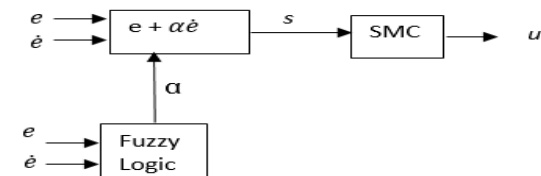
e = y $_{ref}$ − y $_{actual}$ (31)

s = e + k.e   (32)

To get obtain an attractive surface the dynamics usually chosen is

S=m.sign(s)   (33)

Since, the switching caused by the signum function is hard one we replace it by tanh function to make the controller output smoother [13] as shown in the Fig. 9.

6

4. Single-machine system modeling

A single-machine system with an infinite bus (SMIB) has been shown in figure (8).

In this paper, MATLAB software is used for simulating and modeling. Transient stability is studied during the first oscillation, and during this period, the critical clearing time (CCT) will be evaluated. In order to find the critical time of the fault removal, it has been used of step by step method. In this way that the fault duration is gradually increased to obtain the last time in which the system would be unstable. Three-phase fault, which is the worst and most common error in the practical power systems, has been considered for the whole simulations. The fault place is considered on the middle of line *L2*. By this method, CCT has obtained 209 ms for SIMB system without any compensation.

Three-phase fault, which is the worst and most common fault in the practical power systems, has been considered for the whole simulations. The fault place is considered on the *L2*. By this method, CCT has obtained 209 ms for SIMB system without any compensation. It is supposed that the fault has occurred on 7th second after the startup moment; because the system must be reached on the steady state of the permanent performance; otherwise, the shortest fault can also result in the system instability. Now, the method mentioned above, is repeated again to calculate CCT, but this time, UPFC has been placed in the network.
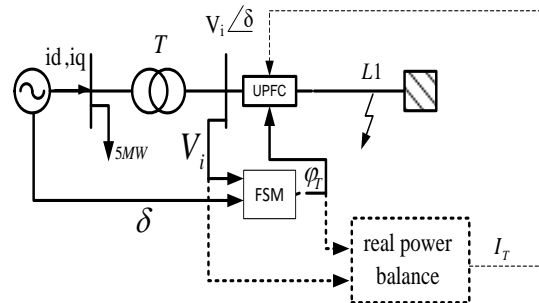

Fig.8. SMIB system with UPFC and controllable blocks

Supposing that UPFC is placed in the network with $V_T = 0.1$ p.u. and $I_q = 0.1$ p.u. Fig. 9 shows a system encountered a three-phase

fault. The results have obtained supposing that the fault has lasted about 230 ms. Figures (9)(a) and (9)(b) show machine angel and machine speed with and without compensator respectively. The main idea of this method is to create the motor orbits under the different primary conditions in mechanical second-degree systems, and then to study the qualitative characteristics of these orbits. Because of being graphical, this method provides a relevant tool for observing the system behavior.

In figures (10)(a) and (10)(b) the speed and angle of the machine with compensator and PI controller and FSM have been respectivey shown in the error duration 230 ms. Figure (10)(a) in same error duration condition, shows the effect of FSM on the other transient stability standards that is the oscillations damping improvement and the overshot reduction.

Figures (11) φ_T obtained from FSM has been shown in order to maximize the energy fanction in the error duration 230 ms.

Table (1) shows CCT values obtained by the various values of V_T , I_q with PI controller and FSM.
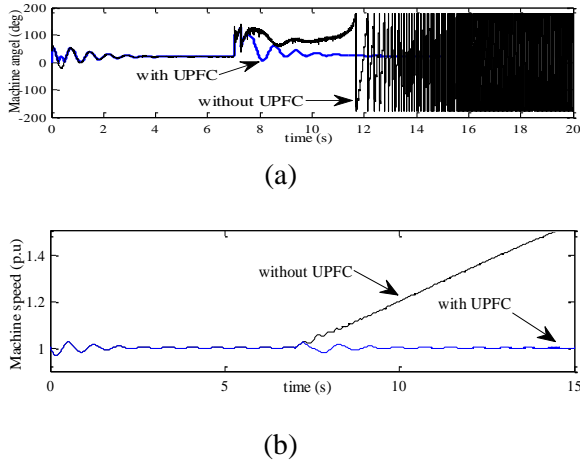

(a)

(b)

Fig. 9. Simulation results of the SMIB with and without UPFC in the error duration 230 ms (a): machine angel (b): machine speed
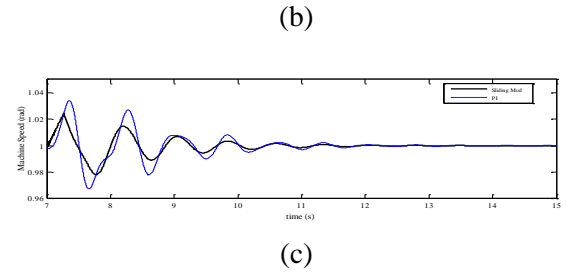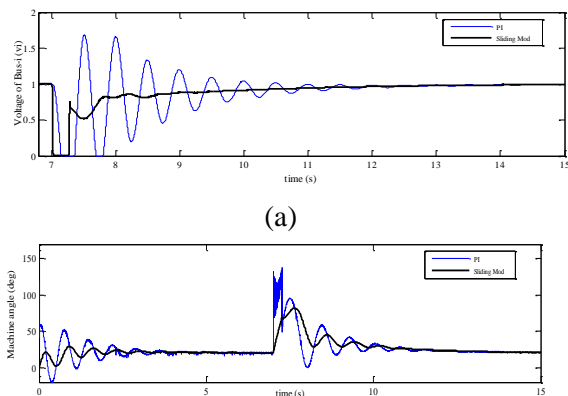

(a)

(b)

(b)

(c)

Fig. 10. Simulation results of the SMIB with UPFC in the error duration 230 ms (a): voltage of bus i (b): machine angel (c): machine speed
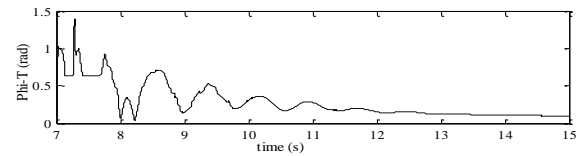

Fig. 11. FSM output in the error duration 230 ms

Table ١: CCTs obtained in a SMIB with different value of U_T including an UPFC

V_T (p.u)	I_q (p.u)	CCT(ms)	
		FSM	PI
0	0	209	209
٠/1	٠/1	248	230
٠/2	٠/1	252	235
0.4	٠/1	258	239

5. Multi-machine system modeling

Standard 9-Bus single line diagram has been shown in Fig.12. Like the single-machine state, by exerting three-phase fault to the system which its place has been shown in Fig.12, by gradual increasing fault time duration, CCT is calculated. For a system without compensation, this time has obtained 117 ms. Here, the fault removal has accommodated by exiting the line from the network, thus, both oscillations and admittance matrix will be different after the fault.
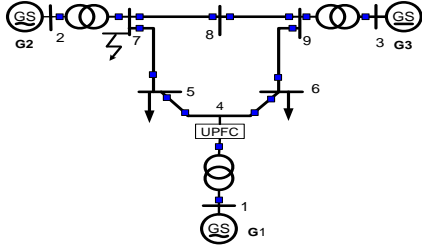
7

Fig.12. 9-Bus single line diagram

When the system, applies UPFC in order to improve the transient stability, it performs as a compensator, its impression must be modeled in some way. Thus, two changes will occur on the main system: first, fault occurrence, and second, entering UPFC to the network. The fault occurrence is modeled by changing the admittance matrix and calculating it on three time periods, and naturally, the power changes. In order to study UPFC in the network, its impression has been directly considered on the network powers. In this manner, the real power injected by UPFC has an impact on the generators' real powers (directly on the generator 1, and indirectly on the other generators), and therefore, it results in improving the operation. In order to compare a system encountered a fault with duration of 129 ms, the system variables have been shown on three conditions in figure (13). In figures (13)(a) and (13)(b) relative angular position and In figures (13)(c) and (13)(d) relative angular speed with and without compensator. Here, this state is similar to the single-machine state in which the system has reached on the steady state, and then, the fault has occurred. Selecting the place has accomplished just by examining two other states, and consequently, the selected place, marked on Fig.12, shows the more CCT increasing toward two other places. UPFC control method, for a multi-machine system, has been exactly considered like a single-machine system to verify its efficiency also for the multi-machine system. Because the methods are alike, it is prevented from the repetition. Emotional Intelligent controllers output, which is the same series branch voltage angle and UPFC power, has been shown on figures (14-a), (14-b) respectively. Table (2) shows CCT values obtained by the various valaes of V_T, I_q with PI controller and FSM.
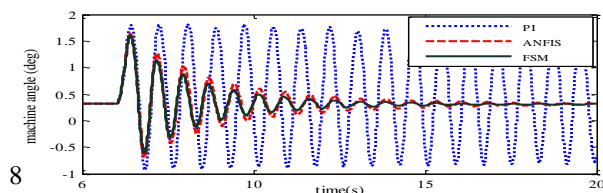
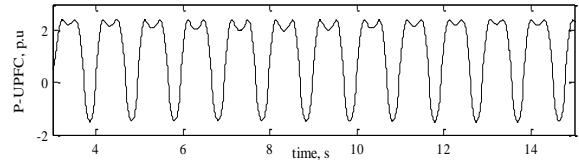(a)
Fig. 13. Simulation results of the 9-buses system with and without compensation in the error duration 129 ms (a): relative angular position δ_{21}
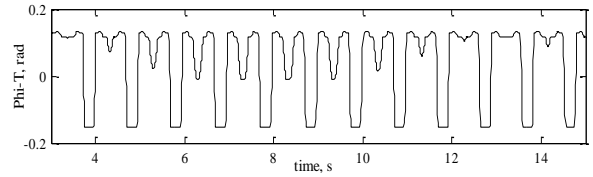
(a)

(b)
Fig. 14. FSM controllers output in the error duration 129 ms (a): φ_T (b): active-power injection by UPFC

Table 2: CCTs obtained in a standard 9-buses system with different value of V_T including an

V_T (p.u)	I_q (p.u)	CCT(ms)	
		FSM	PI
0	0	117	117
0.1	0.1	137	129
0.1	0.4	142	133
0.4	0.1	156	141
UPFC			

Conclusion

In this paper, the transient stability improvement has been studied using UPFC with PI controller and FSM. The application of UPFC with FSM to improve the transient stability is more effective than PI controller. The emotional intelligent controller with a model free and simple structure has a better affect on the oscillation damping, overshot reduction and CCT improvement. Computer simulation tests show the effectiveness and superiority of FSM, in the multi-machine and

single-machine system.

Appendix
Gain parameters for FSMare:
α=1.3e-2, α_{Th}=1.75e-2, β=2.5e-2, $K1$=0.7, $k1$=0.1, $K2$=0. 1, $k2$=0.044, $K3$=0.3, $k3$=0.5.

Multi-machine system data:
Reduced Y matrices:

- Pre-fault network:

$$Y_{R\,pf} = \begin{bmatrix} 0.8455 - 2.989i & 0.287 + 1.513i & 0.21 + 1.226i \\ 0.2871 + 1.513i & 0.4200 - 2.7239 & 0.2133 + 1.09i \\ 0.2096 + 1.226i & 0.2133 + 1.0879 & 0.2770 - 2.3681i \end{bmatrix}$$

- During fault:

$$Y_{R\,df} = \begin{bmatrix} 0.657 - 3.816i & 0 & 0.07 + 0.631i \\ 0 & 0 - 5.4855i & 0 \\ 0.07 + 0.6306i & 0 & 0.1740 - 2.796i \end{bmatrix}$$

- After fault network:

$$Y_{R\,af} = \begin{bmatrix} 1.139 - 2.296i & 0.13 + 0.7063i & 0.1824 + 1.0637i \\ 0.129 + 0.7063i & 0.3745 - 2.0151i & 0.192 + 1.2067i \\ 0.1824 + 1.0637i & 0.192 + 1.2067i & 0.269 - 2.3516i \end{bmatrix}$$

Table 4: Simulation parameters of multi-machine system

Generator no.	1	2	3
Type	Hydro	Steam	Steam
Rated(MVA)	247.5	192	128
(kV)	16.5	18	13.8
Power factor	1	0.85	0.85
Speed(r/min)	180	3600	3600
H	23.64	6.4	3.01
X_d (p.u)	0.164	0.9	1.3125
X'_d (p.u)	0.0608	0.12	0.1813
X_q (p.u)	0.097	0.8645	1.2578
X'_q (p.u)	0.097	0.197	0.25
T_{do} (sec)	8.96	6	5.9
T'_{qo} (sec)	0	0.535	0.6
X_l (p.u)	0.0336	0.0521	0.074

SMIB data:
Table 5: Simulation parameters of SMIB

H (MJ/MVA)	3.12	K_E	-0.245
X_d (p.u)	1.014	T_E (sec)	0.95
X_q (p.u)	0.6	K_F	0.05
X'_d (p.u)	0.314	T_F (sec)	0.35
T'_{do} (sec)	6.55	K_D	2
K_A	400	X_T (p.u)	0.07
T_A (sec)	0.05	X_L (p.u)	0.65

REFERENCES

A. Kumar and S. B. Dubey, "Enhancement of Transient Stability in Transmission Line Using SVC Facts Controller", *International Journal of Recent Technology and Engineering (IJRTE) ISSN: 2277-3878*, Volume-2, Issue-2, May 2013.

M.Karthik and P.Arul, "Optimal Power Flow Control Using FACTS Devices,'' *International Journal of Emerging Science and Engineering (IJESE) ISSN: 2319–6378*, Volume-1, Issue-12, October 2013.

C. Makkar and L. Dewan, "Transient Stability Enhancement using Robust FACTS Controllers- A Brief Tour", *Canadian Journal on Electrical & Electronics Engineering* Vol. 1, No. 7, December 2010.

A. Satheesh and T. Manigandan, "Maintaining power system stability with FACTS controller using bees algorithm and NN", *Journal of Theoretical and Applied Information Technology*, Vol. 49 No.1, 10th March 2013.

S. Krishna, K. R. Padiyar, "Discrete Control of Unified Power Flow Controller for Stability Improvement", Electric Power Systems Research 75, pp. 178-189, 2005.

Narasimhamurthi, M. R. Musavi, "A General Energy Function for Transient Stability Analysis", IEEE Trans. CAS, Vol. CAS-31, No.7, pp. 637-675, July 1984.

Th. V. Cutsem, M. Ribbens-Pavella, "Structure preserving direct methods for transient stability analysis of power systems", Proc. 24th Conf. on Decision and Control, pp 70-77, Dec. 1985.

V. Azbe, U. Gabrijel, D. Povh, R. Mihalic, "The Energy Function of a General Multi-machine System With a Unified Power Flow Controller", IEEE Trans.

Power Systems, Vol. 20, No. 3, August 2005.

M. Januszewski, J. Machowski, J. W. Bialek, "Application of the Direct Lyapunov Method to Improve Damping of Power Swings by Control of UPFC", IEE Proc.-Gener. Transm. Distrib., Vol. 151, No. 2, pp. 252-260, March 2004.

S. Limyingcharoen, U. D. Annakkage, N. C. Pahalawaththa, "Fuzzy Logic Based Unified Power Flow Controllers for Transient Stability Improvement", IEE Proc.-Gener. Transm. Distrib., Vol. 145, No. 3, May 1998.

S.Mishra, "Neural-network-based Adaptive UPFC for Improving Transient Stability Performance of Power System", IEEE Trans. Neural Networks, Vol. 17, No. 2, pp. 461-470, March 2006.

Chia-Chi Chu, Hung-Chi Tsai, "Application of Lyapunov-Based Adaptive Neural Network Controllers for Transient Stability Enhancement," Power and Energy Society General Meeting, pp. 1-6, July 2008.

Taki. F, Abazari. S, Arab Markadeh. G. R," Transient stability improvement using ANFIS controlled UPFC based on energy function" IEEE Conf on Electrical Engineering (ICEE), 2010.

V. K. Chandrakar, A. G. Kothari, "Comparison of RBFN based STATCOM, SSSC and UPFC Controllers for Transient Stability Improvementm," Power Systems Conference and Exposition, pp. 784-791, Nov. 2006.

M. R. Jamaly, A. Armani, M. Dehyadegari, C. Lucas, and Z. Navabi, "Emotion on FPGA: Model driven approach," Expert Syst. Appl., vol. 36,no. 4, pp. 7369–7378, May 2009.

J. Moren, "Emotion and learning: A computational model of the Amygdala," Ph.D. dissertation, Lund Univ., Lund, Sweden, 2002.

G. Shahgholian and A. Movahedi, "Modeling and Controller Design using

ANFIS Method for Nonlinear Liquid Level System", Journal of Information and Electronics Engineering, Vol. 1, No. 3, pp. 271-275, Nov. 2011.

C. Lucas, D. Shahmirzadi, and N. Sheikholeslami, "Introducing FSM:Brain emotional learning based intelligent control," Int. J. Intell. Automat.Soft Comput., Vol. 10, No. 1, pp. 11–22, 2004.

A. Mohanty, M. Viswavandya and P. K. Ray, "An adaptive Fuzzy sliding mode controller for reactive power & transient stability management," 2016 IEEE Region 10 Conference (TENCON), Singapore, 2016, pp. 3195-3199.

H. Rouhani, M. Jalili, B. Arabi, W. Eppler, and C. Lucas, "Brain emotional learning based intelligent controller applied to neurofuzzy model of micro-heat exchanger," Expert Syst. Appl., Vol. 32, No. 3, pp. 911–918,2007.

R. Sivakumar, C. Sahana and P. A. Savitha, "Design of ANFIS-based Estimation and Control for MIMO Systems", Journal of Engineering Research and Applications, Vol. 2, No.. 3, pp. 2803-2809, May-Jun 2012.

M. A. Rahman, R. M. Milasi, C. Lucas, B. N. Arrabi, and T. S. Radwan,"Implementation of emotional controller for interior permanent magnet synchronous motor drive," IEEE Trans. Ind. Appl., Vol. 44, No. 5, pp. 1466-1476, Sep./Oct. 2008.

G. R. Arab Markadeh, E. Daryabeigi, C. Lucas, and M. A. Rahman, "Speed and Flux Control of Induction Motors Using Emotional Intelligent Controller," IEEE Trans. Ind. Appl., Vol. 47, No. 3, pp. 1126-1135, MAY/JUNE 2011.

M. R. Jamali, A. Arami, B. Hosseini, B.Moshiri, and C. Lucas, "Real time emotional control for anti-swing and positioning control of SIMO overhead traveling crane," Int. J. Innovative Comput. Inf. Control, Vol. 4, No. 9, pp. 2333–2344, Sep. 2008.

M. R. Jamali, M. Dehyadegari, A. Arami, C. Lucas, and Z. Navabi, "Realtime embedded emotional controller," J. Neural Comput. Appl., Vol. 19, No. 1, pp. 13–19, 2010.

Arizadayana Z, Irwanto M, Fazliana F, Syafawati AN (2014) Improvement of dynamic power system stability by installing UPFC based on Fuzzy Logic Power System Stabilizer (FLPSS). In: IEEE 8th International Power Engineering and Optimization Conference (PEOCO), pp 188–193.

G. R. Arab Markadeh, E. Daryabeigi, C. Lucas, and M. A. Rahman, "Speed and Flux Control of Induction Motors Using Emotional Intelligent Controller," IEEE Trans. Ind. Appl., Vol. 47, No. 3, pp. 1126-1135, MAY/JUNE 2011.

E. Daryabeigi, G. Arab Markadeh, C. Lucas, "Emotional controller in Electric Drives – A Review", IEEE Conf, IECON 2010, pp. 2901 - 2907 Nov., 2010.

A. R. Sam and P.Arul, "Transient Stability Enhancement of Multi-machine Power System Using UPFC and SSSC", *International Journal of Innovative Technology and Exploring Engineering (IJITEE) ISSN: 2278-3075*, Volume-3, Issue-5, October 2013.

K. Vasudevan, "Maintaining Voltage Stability by Optimal Locating and Sizing by Combined Evolutionary Algorithm, *"International Journal of Computer Applications* 84(12):39-45, Volume 84 - Number 12, December 2013.

A. K. Mohanty and A.K. Barik, "Power System Stability Improvement Using FACTS Devices", *International Journal of Modern Engineering Research (IJMER)*, Vol.1, Issue.2, pp-666-672, ISSN: 2249-6645, May 2012.